



An ultra-thin diamond membrane as a transmission particle detector and vacuum window for external microbeams

V. Grilj, N. Skukan, M. Pomorski, W. Kada, N. Iwamoto, T. Kamiya, T. Ohshima, M. Jakšić

► To cite this version:

V. Grilj, N. Skukan, M. Pomorski, W. Kada, N. Iwamoto, et al.. An ultra-thin diamond membrane as a transmission particle detector and vacuum window for external microbeams. *Applied Physics Letters*, 2013, 103, pp.243106. 10.1063/1.4833236 . cea-01792091

HAL Id: cea-01792091

<https://cea.hal.science/cea-01792091>

Submitted on 3 Mar 2020

HAL is a multi-disciplinary open access archive for the deposit and dissemination of scientific research documents, whether they are published or not. The documents may come from teaching and research institutions in France or abroad, or from public or private research centers.

L'archive ouverte pluridisciplinaire **HAL**, est destinée au dépôt et à la diffusion de documents scientifiques de niveau recherche, publiés ou non, émanant des établissements d'enseignement et de recherche français ou étrangers, des laboratoires publics ou privés.

An ultra-thin diamond membrane as a transmission particle detector and vacuum window for external microbeams

V. Grilj,^{1,a)} N. Skukan,¹ M. Pomorski,² W. Kada,³ N. Iwamoto,⁴ T. Kamiya,⁴ T. Ohshima,⁴ and M. Jakšić¹

¹*Division of Experimental Physics, Ruđer Bošković Institute, 10000 Zagreb, Croatia*

²*CEA-LIST, Diamond Sensors Laboratory, Gif-sur-Yvette F-91191, France*

³*Division of Electronics and Informatics, Faculty of Science and Technology, Gunma University, Kiryu, Gunma 376-8515, Japan*

⁴*Takasaki Advanced Radiation Research Institute, Japan Atomic Energy Agency (JAEA), Takasaki, Gunma 370-1292, Japan*

(Received 18 September 2013; accepted 10 November 2013; published online 11 December 2013)

Several applications of external microbeam techniques demand a very accurate and controlled dose delivery. To satisfy these requirements when post-sample ion detection is not feasible, we constructed a transmission single-ion detector based on an ultra-thin diamond membrane. The negligible intrinsic noise provides an excellent signal-to-noise ratio and enables a hit-detection efficiency of close to 100%, even for energetic protons, while the small thickness of the membrane limits beam spreading. Moreover, because of the superb mechanical stiffness of diamond, this membrane can simultaneously serve as a vacuum window and allow the extraction of an ion microbeam into the atmosphere. © 2013 AIP Publishing LLC. [<http://dx.doi.org/10.1063/1.4833236>]

The ability of microprobe facilities to extract an ion microbeam outside a vacuum system provides a valuable tool for the investigation of localized radiation effects in samples that are unsuitable for mounting inside the vacuum chamber. Among others, these samples include live biological specimens that cannot survive high-vacuum conditions and detectors or other semiconductor setups that are too large to fit inside the chamber. To achieve a precise delivery of a known dose of radiation to each sample, a charged-particle detection system with high sensitivity is of the utmost importance. The realization of such a system at an external microprobe facility presents a real challenge when the energy of the ion is not sufficient to penetrate the whole sample thickness. In that case, the need for an appropriate transmission detector emerges.

Two different transmission-detector setups are primarily used for external microbeams. One is based on the detection of the secondary electrons that are emitted from the vacuum exit foil when an ion passes by.^{1–3} While such a device can achieve a hit-detection efficiency of close to 100% for heavier ions, the efficiency is significantly lower for light ions. The other commonly used setup relies on ion detection using thin scintillation foils.^{4,5} Although characterized by a higher sensitivity to light ions, this option requires total darkness at the irradiation stage, which prevents the observation of the sample during irradiation.

Here, we propose a detection setup that consists of an ultra-thin single-crystal chemical-vapor-deposited (scCVD) diamond membrane used simultaneously as a single-hit transmission detector and a vacuum window. This device could potentially overcome the problems mentioned above.

A self-supported diamond membrane of approximately 6 μm in thickness was produced from cheap, so-called

optical-grade (substitutional nitrogen content $[\text{N}] < 1$ ppm), scCVD diamond using the argon/oxygen plasma etching technique. Afterward, the sample was metalized in a parallel-plate geometry via sputtering of 300 nm thick Al contacts. More details concerning the detector fabrication procedure can be found in Ref. 6. The detector was suspended over a 1.5 mm hole drilled into a brass flange (ISO KF16 standard) and glued with a conductive epoxy, which electrically connected the back electrode to the flange. The connection to the electronic chain was provided by the SMA connector soldered onto the flange [Fig. 1(a)].

Additional information regarding the current-voltage and capacitance-voltage characteristics of the produced detector will be provided elsewhere and are not within the scope of this paper.

The detector performances were first evaluated in a high-vacuum environment. For that purpose, the entire flange with the membrane attached was mounted on the sample holder inside the vacuum chamber at the RBI microprobe line,⁷ and the output signal from the detector was fed first into a charge-sensitive preamplifier (ORTEC model 142a) and then into a shaping amplifier (ORTEC model 572a). After amplification, the pulses were analyzed using an analog-to-digital multichannel analyzer (ADC-MCA) and the data-acquisition software SPECTOR.⁸ A commercial

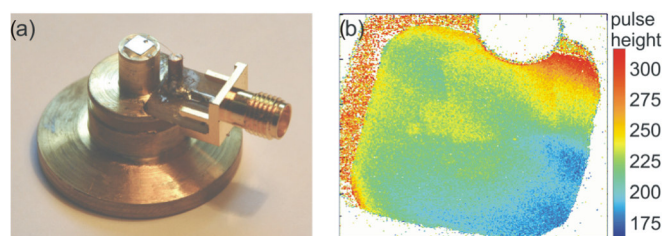


FIG. 1. (a) The final detector setup. (b) An IBIC image of the diamond membrane.

^{a)} Author to whom correspondence should be addressed. Electronic mail: vgrilj@irb.hr. Tel.: +385 1 457 1254, Fax: +385 1 4680 239.

300- μm -thick scCVD diamond detector (purchased from CIVIDEC Instrumentation) was connected to an identical electronic chain and placed less than 2 mm behind the membrane, thereby forming a ΔE -E configuration. With this experimental setup, several detector characteristics were investigated as follows:

- (1) Variations in the membrane thickness were observed using ion-beam-induced charge (IBIC) imaging. In an IBIC image, the average pulse height in each pixel is represented by the appropriate color on a color scale. A microbeam of 1.3 MeV protons with a spot size of less than 1 μm was scanned over the front side of the detector (biased at 42 V, electric field $\approx 7\text{ V}/\mu\text{m}$), and the IBIC image shown in Fig. 1(b) was recorded. Areas of the device that exhibit a higher induced signal correspond to a higher energy loss of the incident beam caused by a greater thickness of the membrane. From energy-loss measurements and using SRIM⁹ calculations, we were able to estimate that the thickness of the etched part varied from 5.3 up to 5.9 μm , which was most likely caused by some initial non-parallelism of the diamond plate and by mechanical polishing.
- (2) To investigate the charge-collection efficiency (CCE) of our device, which is defined as the ratio of the amount of charge collected at the electrodes (Q) to the amount of charge created inside the detector (Q_0), the signal amplitude of the 1.3 MeV protons was measured using the membrane (biased at 42 V) and using the commercial diamond detector (biased at 300 V) with and without the membrane in the way [Fig. 2(a)]. Considering the energy deposited inside the metal layer of the electric contacts and assuming that the energies required to produce an electron-hole pair in the diamond membrane and in the commercial diamond detector are equal, we calculated the CCE of the membrane to be greater than 99%, despite the contamination of the diamond crystal with nitrogen. In addition, the behavior of the CCE as a function of the electric field was measured for bias voltages from 42 V down to 1 V with both polarities [Fig. 2(b)].
- (3) To obtain an estimate of the amount of beam broadening that can be expected because of the scattering of ions from the carbon atoms in the membrane, a copper mesh with a pitch of 25 μm was imaged via scanning transmission ion microscopy (STIM) using the commercial diamond detector with and without the beam having passed through the membrane first. We used an

older membrane sample that was produced in the same way and with a similar thickness (approximately 6 μm). This sample was accidentally broken, which actually made it easier to attach the copper mesh behind it. The distance between the mesh and the broken membrane was approximately 150 μm . The 2 MeV proton beam was scanned over the edge of the broken diamond membrane in such a way that on one part of the scanning area, the protons were directly incident on the mesh [Fig. 3(a)], while on the other part, they penetrated the membrane first [Fig. 3(b)]. The membrane caused an increase in the beam width from 1.4 to 2.6 μm . One should bear in mind that the amount of broadening is strongly dependent on the distance between the membrane and the sample and this distance should be reduced as much as possible.

- (4) Radiation hardness is an important feature of detectors that are used in high-radiation environments. Although our previous work¹⁰ indicated that the superb durability of diamond over silicon under irradiation by protons in the GeV energy range¹¹ cannot be simply extrapolated to MeV protons, diamond still exhibits the great advantage of a negligible leakage current that does not change with the level of irradiation.¹¹ To check the radiation tolerance of our device, we selectively irradiated six areas ($100 \times 100\text{ }\mu\text{m}^2$) with different fluences of 1.3 MeV protons [Fig. 4(a)] and measured the normalized induced charge, defined as the ratio Q_0/Q , at each area. The results are shown in Figure 4(b), alongside the data obtained in a similar measurement for a commercial 50- μm -thick scCVD diamond detector (purchased from Diamond Detectors Ltd.), on which damaged areas

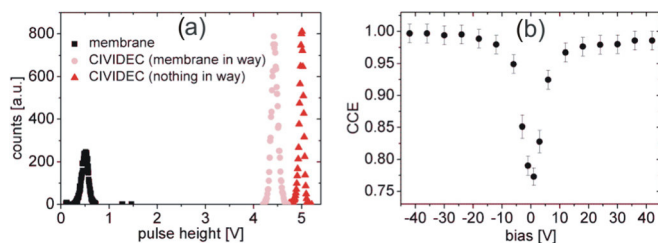


FIG. 2. (a) Pulse-height distributions of 1.3 MeV protons recorded for the diamond membrane and for the commercial diamond detector with (pink dots) and without (red triangles) the membrane in the way. (b) Dependence of the membrane's CCE on the bias voltage.

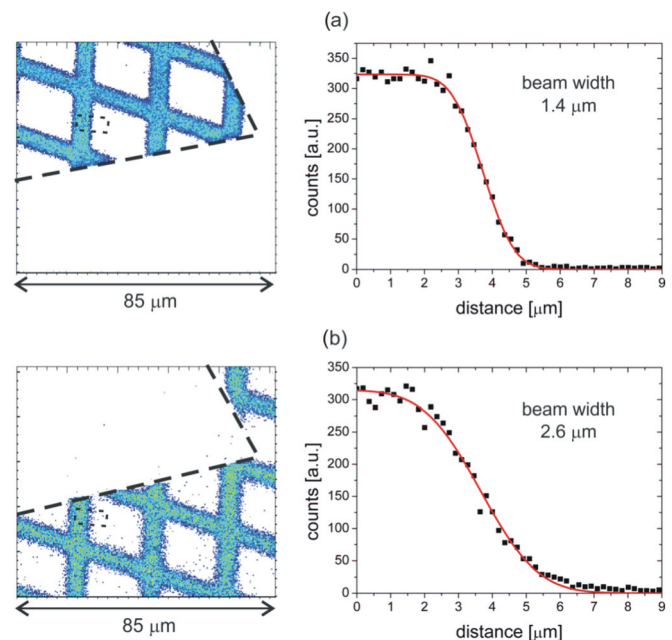


FIG. 3. STIM images of a copper grid (25 μm pitch) bombarded with 2 MeV protons: (a) directly incident on the grid and (b) first passing through a broken diamond membrane. The black segmented line shows the edge of the broken membrane. The small dotted squares indicate areas from which distributions of the number of projected counts were obtained and plotted on the right. These distributions were fitted to the error function, and the beam width was estimated as the distance between 10% and 90% of the error-function plateau in both cases.

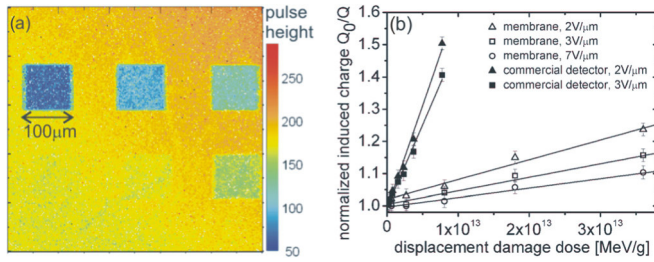


FIG. 4. (a) An IBIC image showing six areas of the diamond membrane that were purposely damaged by irradiation with different doses of 1.3 MeV protons. (b) Dependence of the normalized induced charge (Q_0/Q) on the displacement damage dose for the diamond membrane and for the 50-μm-thick commercial diamond detector. Data are shown for electric fields of 2 and 3 V/μm (both detectors) and for 7 V/μm (only membrane). The continuous lines represent the least-squares fits of the experimental values to Eq. (1).

were produced using 4.5 MeV protons to maintain homogeneous vacancy production throughout the bulk of the detector. The commercial detector serves as a reference in this case. To compare the CCE degradation, a non-ionizing energy loss (NIEL) concept¹² was used as a measure of the lattice defects introduced into a material by different ions, and both data sets were fitted to a simple phenomenological equation

$$\frac{Q_0}{Q} = 1 + K_{ed} \times D_d, \quad (1)$$

where K_{ed} represents the equivalent damage factor,¹³ which can serve as a measure of the radiation hardness of the tested material (smaller values of K_{ed} mean better radiation hardness), and D_d is known as the displacement damage dose, which is equal to the product of the absolute fluence and the amount of NIEL. The calculated values of K_{ed} are shown in Table I.

The higher radiation hardness of the membrane in comparison to the commercial diamond detector is a consequence of the much shorter collection distance of the charge carriers. Hence, the time required for the electrons and holes to reach the electrodes for the same electric field is reduced, and the probability of them becoming trapped by energy levels associated with the lattice defects produced by the irradiation also decreases. Moreover, the highest electric field that can be applied to the membrane without sparking is approximately 7 V/μm and greatly exceeds the field that can be applied to the 50-μm-thick commercial diamond detector. Operating the membrane at so high electric field enhances its resistivity to radiation [Fig. 4(b)]. The effects of polarization, which often causes a large unexpected decrease in the signal output of diamond detectors¹⁴ and is closely related to defects inside the material, were not observed.

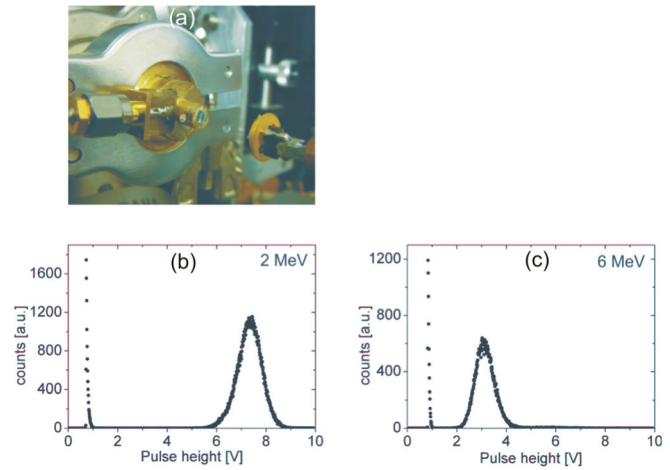


FIG. 5. (a) The membrane mounted on the microprobe chamber as a vacuum window, (b) 2 MeV protons and (c) 6 MeV protons recorded for the diamond membrane. The noise edge is intentionally shown on the left-hand side of both spectra to display its separation from the signal.

After all vacuum tests were performed, the membrane detector was installed on the microprobe chamber as a vacuum/air interface [Fig. 5(a)]. The basic vacuum of the chamber was achieved, and bending of the membrane caused by the high pressure difference was clearly visible. To check the operability of the detector in these conditions, we connected it to an electronic chain such as the one described before, with the exception of the preamplifier, for which a CoolFET A250CF was used instead of an ORTEC 142a to reduce the electronic noise. Energetic protons were selected as the probe because they are the most critical ion species for detection. Spectra of 2 and 6 MeV protons were recorded with an ion rate of 500 Hz and are shown in Figs. 5(b) and 5(c). The signals are well separated from the noise in both cases.

The hit-detection efficiency was calculated by comparing the number of pulses from the silicon PIN diode, which was placed behind the diamond membrane in air, to the number of coincident pulses from the membrane and the diode for 6 MeV protons. Bipolar outputs from both detectors were fed into single-channel analyzers (SCA) operating in crossing-over mode and then into a time-to-amplitude converter (TAC). All events from the TAC were grouped into a peak with a FWHM of less than 1 μs, which confirmed that they were coincident, as no fast electronics was employed. A digital counter was used to count the TAC pulses and the output pulses from the diode's SCA simultaneously. The measurement was repeated for ion rates ranging from a few tens of Hz to 1 kHz. The calculated hit-detection efficiency exceeded 99%, regardless of the ion rate. This was the final confirmation that the device can operate as an efficient transmission detector and, at the same time, withstand high vacuum conditions.

TABLE I. Calculated values of the equivalent damage factor K_{ed} obtained from the IBIC results for a partially damaged diamond membrane and a 50-μm-thick commercial diamond detector, measured at electric fields of 2 and 3 V/μm (both detectors) and 7 V/μm (only membrane).

Electric field	2 V/μm		3 V/μm		7 V/μm
	Diamond membrane	Commercial detector	Diamond membrane	Commercial detector	Diamond membrane
$K_{ed} (\times 10^{-15} \text{ g/MeV})$	6.1 ± 0.1	62 ± 2	4.2 ± 0.1	50 ± 1	2.91 ± 0.08

The concept investigated in our work has several advantages over the conventional setups. The greatest advantage in comparison with devices that record the secondary electrons emitted by ion passage is its excellent hit-detection efficiency for energetic light ions, which arises from the negligible intrinsic noise of diamond. The operation of our device is also considerably simpler than the operation of scintillation detectors, and it does not prevent the simultaneous observation of the sample. Moreover, the ability to install the detector as a vacuum window reduces the need for an additional exit foil and enables the minimization of the distance between the membrane, which is a source of beam broadening, and the sample. This plays a crucial role in maintaining the appropriate spatial resolution for experiments that require sub-micron beam spots. The combination of the above features makes this detector highly appropriate for experiments that require fast and reliable triggering, such as live cell irradiations or single-event upsets. In addition, the outstanding results of the radiation-hardness test indicate a wider possible range of device applications, including those that involve high currents of charged particles or long exposure to radiation. However, a significant amount of energy loss for heavy ions (heavier than protons) makes the detector inadequate in cases when the straggling in ion energy should be minimized or when the achieving of sufficient ion energy is not possible.

This work was supported by the Japanese-Croatian Cooperative Research Project “Development of high-energy

ion microbeam technology for novel applications of diamond.”

- ¹B. E. Fischer, M. Cholewa, and H. Noguchi, *Nucl. Instrum. Methods Phys. Res. B* **181**, 60 (2001).
- ²T. Kamiya, M. Cholewa, A. Saint, S. Prawer, G. J. F. Legge, J. E. Butler, and D. J. Vesteyck, Jr., *Appl. Phys. Lett.* **71**, 1875 (1997).
- ³R. W. Smith, M. Karlušić, and M. Jakšić, *Nucl. Instrum. Methods Phys. Res. B* **277**, 140 (2012).
- ⁴M. Folkard, B. Vojnovic, G. Schettino, M. Forsberg, G. Bowey, K. M. Prise, B. D. Michael, A. G. Michette, and S. J. Pfauntsch, *Nucl. Instrum. Methods Phys. Res. B* **130**, 270 (1997).
- ⁵Ph. Moretto, C. Michelet, A. Balana, Ph. Barbaret, W. J. Przybylowicz, J. P. Slabbert, V. M. Prozesky, C. A. Pineda, G. Brut, G. Laurent, and F. Lhoste, *Nucl. Instrum. Methods Phys. Res. B* **181**, 104 (2001).
- ⁶M. Pomorski, B. Caylar, and P. Bergonzo, *Appl. Phys. Lett.* **103**, 112106 (2013).
- ⁷M. Jakšić, I. Bogdanovic-Radovic, M. Bogovac, V. Desnica, S. Fazinic, M. Karlusic, Z. Medunic, H. Muto, Z. Pastuovic, Z. Siketic, N. Skukan, and T. Tadic, *Nucl. Instrum. Methods Phys. Res. B* **260**, 114 (2007).
- ⁸M. Bogovac, I. Bogdanović, S. Fazinić, M. Jakšić, L. Kukec, and W. Wilhelm, *Nucl. Instrum. Methods Phys. Res. B* **89**, 219 (1994).
- ⁹J. F. Ziegler, J. B. Biersack, and U. Littmark, *SRIM—The Stopping and Range of Ions in Solids* (Pergamon Press, New York, 1985).
- ¹⁰V. Grilj, N. Skukan, M. Jakšić, W. Kada, and T. Kamiya, *Nucl. Instrum. Methods Phys. Res. B* **306**, 191 (2013).
- ¹¹The RD42 Collaboration, *Nucl. Instrum. Methods Phys. Res. A* **426**, 173 (1999).
- ¹²S. R. Messenger, E. A. Burke, G. P. Summers, M. A. Xapsos, R. J. Walters, E. M. Jackson, and B. D. Weaver, *IEEE Trans. Nucl. Sci.* **46**, 1595 (1999).
- ¹³F. W. Sexton, K. M. Horn, B. L. Doyle, M. R. Shaneyfelt, and T. L. Meisenheimer, *IEEE Trans. Nucl. Sci.* **42**, 1940 (1995).
- ¹⁴M. Guthoff, K. Afanaciev, A. Dabrowski, W. de Boer, W. Lange, W. Lohmann, and D. Stickland, *Nucl. Instrum. Methods Phys. Res. A* **730**, 168–173 (2013).